An Intercellular Heme-Trafficking Protein Delivers Maternal Heme to the Embryo during Development in *C. elegans*

Caiyong Chen,[1] Tamika K. Samuel,[1,3] Jason Sinclair,[1,3] Harry A. Dailey,[2] and Iqbal Hamza[1,*]

[1]Department of Animal & Avian Sciences and Department of Cell Biology & Molecular Genetics, University of Maryland, College Park, MD 20742, USA
[2]Biomedical and Health Sciences Institute, Department of Microbiology and the Department of Biochemistry and Molecular Biology, University of Georgia, Athens, GA 30602, USA
[3]These authors contributed equally to this work
*Correspondence: hamza@umd.edu
DOI 10.1016/j.cell.2011.04.025

SUMMARY

Extracellular free heme can intercalate into membranes and promote damage to cellular macromolecules. Thus it is likely that specific intercellular pathways exist for the directed transport, trafficking, and delivery of heme to cellular destinations, although none have been found to date. Here we show that *Caenorhabditis elegans* HRG-3 is required for the delivery of maternal heme to developing embryos. HRG-3 binds heme and is exclusively secreted by maternal intestinal cells into the interstitial fluid for transport of heme to extraintestinal cells, including oocytes. HRG-3 deficiency results either in death during embryogenesis or in developmental arrest immediately post-hatching—phenotypes that are fully suppressed by maternal but not zygotic *hrg-3* expression. Our results establish a role for HRG-3 as an intercellular heme-trafficking protein.

INTRODUCTION

Heme-containing proteins are found in nearly all phyla of organisms (Hardison, 1996) and play essential roles in a wide range of biological process (Faller et al., 2007; Kaasik and Lee, 2004; Okano et al., 2010; Severance and Hamza, 2009). In mammalian cells, heme is either imported from the extracellular milieu through the plasma membrane (Uc et al., 2004; Worthington et al., 2001) or synthesized within the mitochondria for export to the cytoplasm for delivery to extramitochondrial compartments for insertion into a repertoire of hemoproteins (Dailey, 2002; Severance and Hamza, 2009). Free heme is an amphipathic planar macrocycle that can intercalate into membranes where it may promote damage to cellular macromolecules (Balla et al., 1991). Consequently, specific cellular pathways must exist for the directed transport, trafficking, and delivery of heme to numerous cellular destinations—but none have been found to date (Severance and Hamza, 2009). Previously, we identified

the first bona fide metazoan heme importer HRG-1 (SLC48A1), which we propose plays a critical role in regulating cellular heme homeostasis in the roundworm *Caenorhabditis elegans* and vertebrates (Rajagopal et al., 2008). Heme export is mediated by a major facilitator superfamily protein, the feline leukemia virus subgroup C cellular receptor (FLVCR), in red blood cells and macrophages (Keel et al., 2008; Quigley et al., 2004). Hemopexin, a serum heme-binding protein, may facilitate heme export by physically interacting with FLVCR (Yang et al., 2010). Together, these proteins constitute part of a larger, intricate network to maintain organismal heme homeostasis—a concept heretofore poorly understood (Severance et al., 2010).

In an effort to identify additional components of the heme transport pathways, we took advantage of *C. elegans*, a heme auxotroph (Rao et al., 2005). In worms, nutritional heme is transported into the intestine by membrane-bound permeases—HRG-1 and HRG-4 (Rajagopal et al., 2008). However, it's unclear how tissues such as muscle, neurons, hypodermal cells, and embryos acquire heme from the intestine. Here we identify HRG-3, a heme-binding protein that functions to transport heme from intestinal cells to extraintestinal tissues including oocytes. Our results suggest that HRG-3 is an intercellular heme carrier that is essential for early development in *C. elegans*.

RESULTS

Embryonic Heme Levels Are Affected by Maternal Heme Availability

C. elegans wild-type N2 worms maintained axenically in mCeHR-2 liquid medium are gravid adults in 3.5 days in the presence of optimal concentrations of heme (20 μM) (Rao et al., 2005). However, their progeny are growth arrested at the fourth larval stage (L4) in the absence of supplemented heme. To differentiate the effects mediated by maternal heme from zygotic heme, we cultured parental worms (P_0) at 1.5, 20, and 750 μM heme, all of which allow normal development and fertility, and the ensuing progeny (F_1) were maintained at either 0 or 20 μM heme (Figure 1A and Figure S1 available online). Strikingly, when grown at 0 μM heme, F_1 worms obtained from P_0 mothers cultured at 1.5 μM heme were growth arrested at the first larval
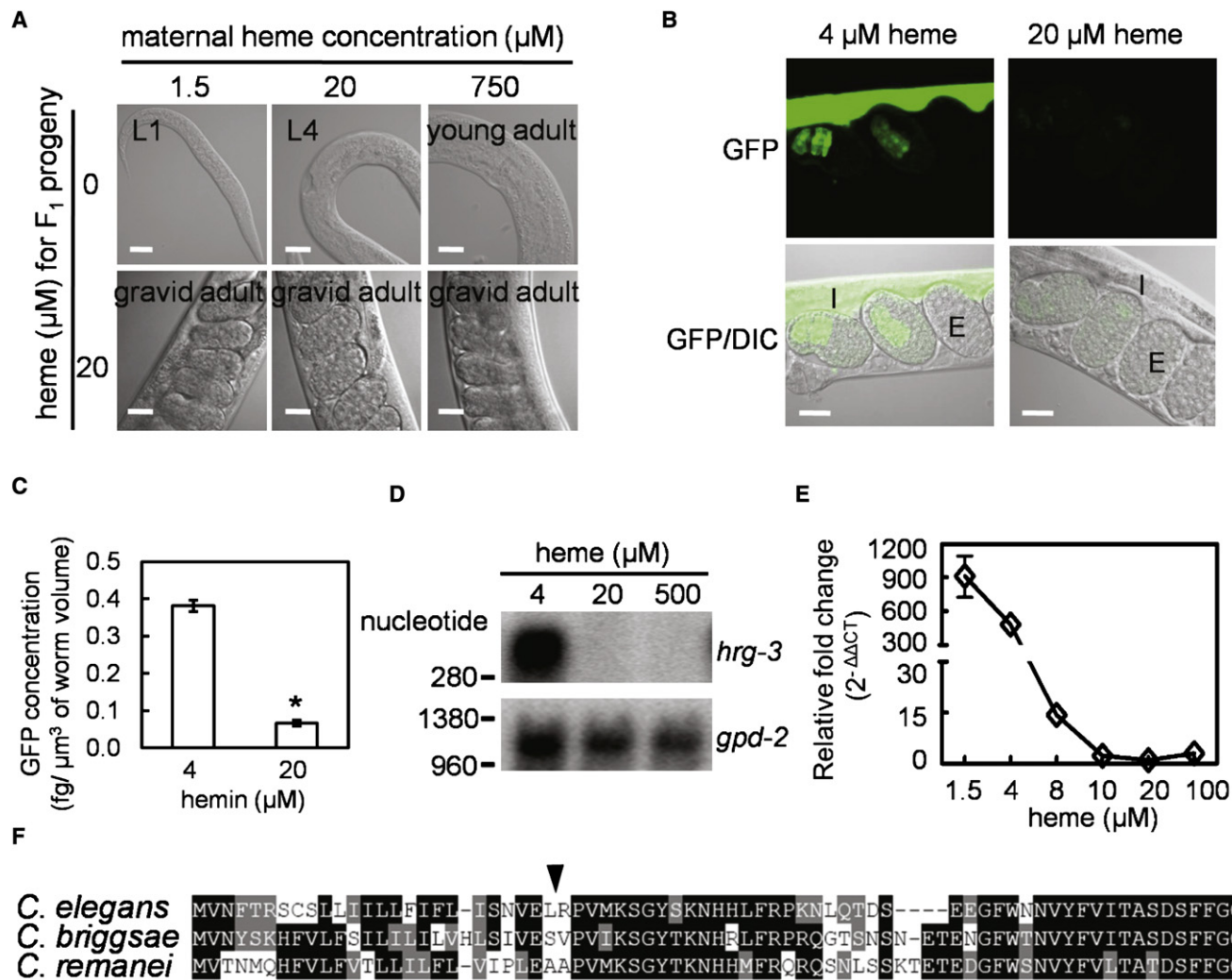
Figure 1. *hrg-3* Is Induced by Heme Deficiency in *C. elegans*

(A) Parental worms were grown at the indicated heme concentrations for one generation, and the synchronized L1 (first stage larvae) progeny were inoculated into axenic mCeHR-2 medium supplemented with 0 or 20 μM heme. Representative images of the progeny at day 5 are shown. L4, the fourth stage of larvae. Scale bar, 20 μm.

(B) Environmental heme represses the expression of both maternal and embryonic GFP in the heme sensor strain IQ6011. I, maternal intestine; E, embryos. Scale bar, 20 μm.

(C) GFP fluorescence quantification in the embryos derived from IQ6011 grown at 4 and 20 μM heme. Error bars represent SEM from three independent experiments. *p < 0.001 compared with 4 μM heme.

(D) Northern blot analysis of *hrg-3* (~370 nucleotides) expression using total RNA isolated from worms grown at different heme concentrations. The blot was reprobed with the internal control *gpd-2*.

(E) Quantification of *hrg-3* mRNA by qRT-PCR. Relative fold changes were derived by normalizing the cycle threshold values to *gpd-2* and then to samples derived from 20 μM optimal heme using the ΔΔCT method. The experiment was performed in triplicate, and the error bars indicate SEM.

(F) Comparison of HRG-3 proteins in *C. elegans*, *C. briggsae*, and *C. remanei*. Arrowhead, putative signal peptidase cleavage site and underline, hydrophobic leader peptide.

See also Figure S1 and Table S2.

stage (L1), whereas F_1 worms derived from P_0 worms grown at 750 μM heme grew to young adults prior to becoming growth arrested. Irrespective of the P_0 heme concentrations, F_1 progeny developed normally when grown at 20 μM heme (Figure 1A and Figure S1). These results suggest that larval development after hatching is dependent upon maternal (P_0) deposition of heme,

and that in the presence of heme, the F_1 progeny can overcome maternally induced heme deficiency.

To corroborate these results, we used a transgenic heme sensor strain in which the expression of intestinal GFP is inversely correlated with heme levels in the worm (Sinclair and Hamza, 2010). When worms were maintained at low

concentrations of heme, strong GFP expression was observed both in the maternal intestine and in the embryos. However, embryonic GFP expression was severely attenuated, concomitant with maternal GFP, when mothers were provided with 20 μM heme, further demonstrating that heme levels in the embryos are linked to maternal heme status (Figures 1B and 1C).

Heme Deficiency Induces *hrg-3* Expression in *C. elegans*

A previous transcriptome analysis identified several hundred heme-responsive genes (*hrg*s) in worms grown in axenic mCeHR-2 liquid culture supplemented with 4, 20, and 500 μM heme (Severance et al., 2010). To identify genes that may play a role in heme delivery, we first sorted genes based on the degree of upregulation under low heme conditions followed by three additional criteria. They should encode proteins (1) with a molecular weight of $\leq$30 kDa—a feature characteristic of metallochaperones (Kim et al., 2008), (2) with conserved amino acids that bind heme (H, Y, or C), and (3) that lack multispan transmembrane domains. These criteria resulted in the identification of F58E6.7, which was upregulated >70-fold by low heme in the microarray. Northern blot analysis revealed the presence of a single ~370 nucleotide transcript (Figure 1D), and qRT-PCR revealed that worms grown in 1.5 or 4 μM heme increased the abundance of F58E6.7 mRNA by more than 900-fold and 400-fold, respectively, over what is found in worms grown in 20 μM heme (Figure 1E). Consistent with the northern blotting results, 5′ and 3′ RACE confirmed the presence of an ~377 nucleotide mRNA containing an ~9 nucleotide 5′ untranslated region (UTR), three exons, and a 155 nucleotide 3′ UTR (not shown). The open reading frame (ORF) encodes a 70 amino acid protein with a predicted molecular mass of 8.1 kDa (Figure 1F). Within the amino terminus of F58E6.7 resides a stretch of hydrophobic amino acids, which could serve as either a transmembrane region or a signal peptide. BLAST searches and gene prediction algorithms identified putative homologs in other *Caenorhabditis* species (Figure 1F). These homologs share >50% sequence identity at the amino acid level. Consistent with genome nomenclature, we termed F58E6.7 as *hrg-3*.

Lack of *hrg-3* in *C. elegans* Reveals Developmental Phenotypes during Heme Deficiency

To determine the function of HRG-3 in *C. elegans*, we analyzed worms containing a deletion in *hrg-3*. The *tm2468* strain contains a 218 bp deletion that encompasses part of the promoter, the first two exons and the first intron, resulting in a null mutant (Figures 2A and 2B). These mutant worms have no overt phenotypes when fed the standard worm diet containing *E. coli* strain OP50 (not shown). Because *hrg-3* is highly upregulated in worms grown at low heme conditions in mCeHR-2 liquid medium, and to rigorously analyze the *hrg-3* mutant phenotype, we sought to recapitulate the heme deprivation conditions on agar plates with *E. coli* as the food source. Because the OP50 *E. coli* strain can synthesize heme endogenously, it was not possible to deplete the bacteria of heme. The bacterial strain RP523 is defective in *hemB*, which encodes 5-aminolevulinic acid dehydratase (ALAD), the second enzyme in the heme biosynthesis pathway (Li et al., 1988). Consequently, RP523 is dependent upon exogenous heme for growth. By exposing worms to RP523 grown with different concentrations of heme, one can control heme levels in the worm via *E. coli*. Wild-type N2 worms exhibited a 1 to 2 day growth delay when fed RP523 grown with 1 μM heme compared to those grown on OP50, a growth phenotype that was not present when wild-type worms were fed RP523 grown with 10 to 50 μM heme (not shown). *hrg-3* mutant worms, like wild-type worms, revealed the expected growth delay in the parental (P_0) generation when fed RP523 grown with 1 μM heme. However, ~40% of eggs laid by the mutant worms failed to hatch (Figure 2C), and the F_1 embryos that did hatch were growth arrested at the first larval stage (Figures 2D and 2E). The lethality and growth retardation phenotypes were completely rescued when *hrg-3* mutants were fed RP523 that had been grown with 50 μM heme. Collectively, these results indicate that HRG-3 is essential for both embryonic and postembryonic development under heme-limiting conditions and that the absence of HRG-3 results in heme deficiency that is manifested specifically in the F_1 generation.

HRG-3 Is Secreted by the Intestine into the Interstitial Fluid

We determined the tissue and subcellular distribution of HRG-3. Worms expressing *Phrg-3::GFP* transcriptional fusions had GFP in the worm intestine, with the greatest levels in the anterior (int2 and int3) and mid-intestinal cells (int4–6). The anterior-most (int1) and the posterior-most gut cells (int7–9) possessed low levels of GFP (Figure 3A). GFP was only observed in worms that were maintained in $\leq$6 μM heme in mCeHR2 medium—consistent with the qRT-PCR results (not shown). Intestinal *Phrg-3::GFP* expression was observed through all larval stages, and in both hermaphrodites and males (Figure S2). Zygotic expression of *hrg-3* was first detected in late embryos at ~300 min of development (Figure S2).

To identify the subcellular distribution of HRG-3, we constructed transgenic worms that express the translational reporter *Phrg-3::HRG-3::YFP*. Worms grown in 2 μM heme possessed a weak HRG-3::YFP signal that was located in cytoplasmic puncta within the worm intestine (Figure 3B, left panel). Unexpectedly, the majority of HRG-3::YFP was present as vesicular structures outside the intestine in coelomocytes—macrophage-like scavenger cells located in the pseudocoelomic cavity (Figure 3B, right panel).

To determine whether the *HRG-3::YFP* translational reporter was inadvertently expressed in extraintestinal cells, we directed the expression of *hrg-3* from the *vha-6* promoter, a well-characterized intestinal promoter (Oka et al., 2001). Transgenic worms expressing *Pvha-6::HRG-3::mCherry* revealed strong HRG-3::mCherry localization in extraintestinal tissues including coelomocytes, the pseudocoelom, gonadal sheath cells, and the uterus (Figure 3C). Within intestinal cells, HRG-3::mCherry signal was observed as distinct cytoplasmic vesicles that colocalized with mannosidase::GFP (Mans-GFP), a protein that localizes to the Golgi (Figure 3D). However, unlike HRG-3::mCherry, expression of Mans-GFP from the *vha-6* promoter showed no extraintestinal localization (Figure 3D). Taken together, these results strongly suggest that HRG-3 is secreted from the intestinal cells into the pseudocoelom for uptake by extraintestinal tissues.
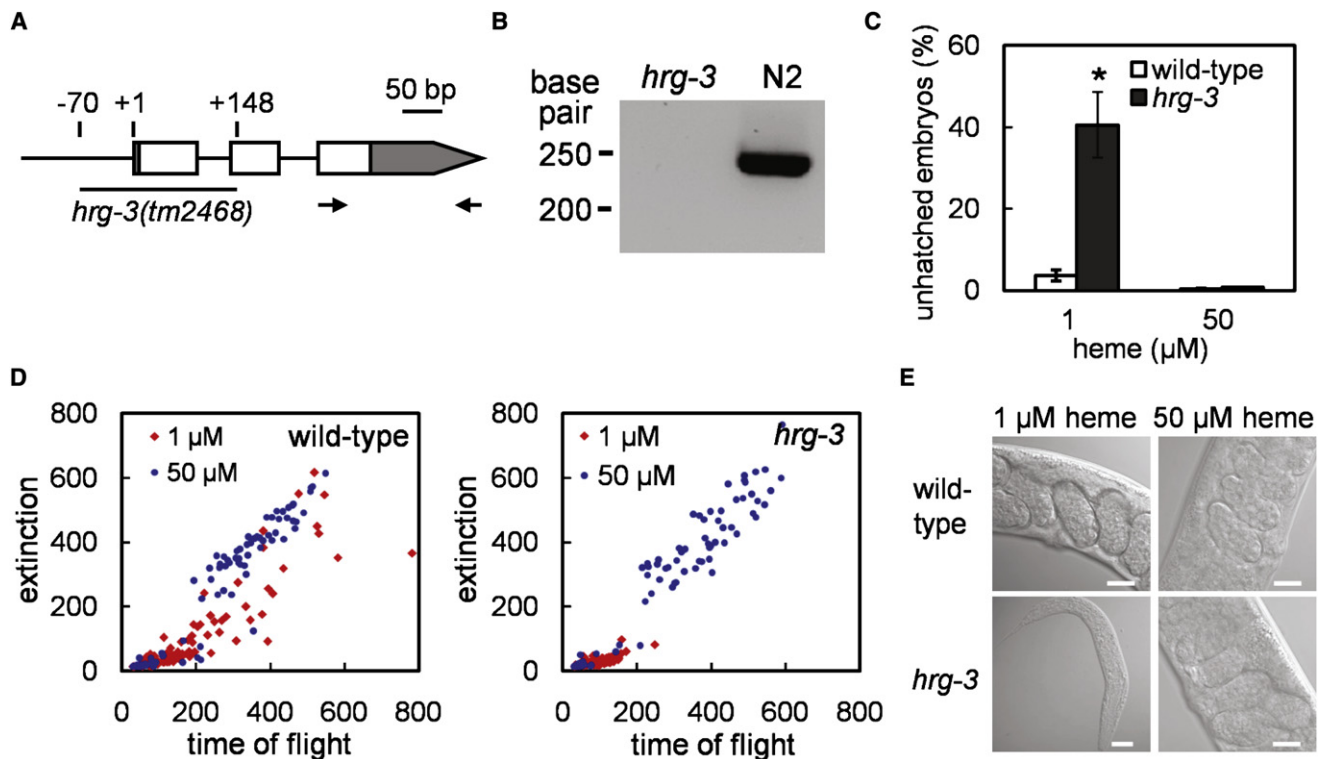
Figure 2. *hrg-3* Is Required for Early Development under Low Heme

(A) *hrg-3* contains three exons. The deleted region in *tm2468* allele is depicted by an underline. Open rectangles, exons; gray boxes, untranslated regions; +1, transcription start site.

(B) RT-PCR was performed using the primer set shown as arrows in Figure 2A on total RNA extracted from the *hrg-3* (*tm2468*) and N2 (wild-type control) worms grown at low heme.

(C) *hrg-3* mutants and their wild-type broodmates were fed with heme-deficient strain RP523 grown at the indicated heme concentrations. Percentage of unhatched embryos were scored following incubation at 20°C for 24 hr. Error bars indicate the SEM from three individual experiments. *$p < 0.001$ compared with wild-type broodmate controls under the same condition.

(D) Worm strains were grown on RP523 for two subsequent generations. F_1 worms were sorted by COPAS BioSort. Time of flight and extinction indicate the length and the optical density of worms, respectively.

(E) Progeny grown on RP523 with 1 and 50 μM heme were imaged at day 6 and day 3 post-hatching, respectively. Representative images of gravid adults in controls and the arrested larvae of *hrg-3* mutants are shown. Scale bar, 20 μm.

HRG-3 Is Specifically Targeted to the Secretory Pathway

To determine whether HRG-3 is a membrane-anchored protein within an exosome or a soluble secreted protein, we synthesized truncated variants of HRG-3 that were tagged at the C terminus with GFP. Expression of HRG-3-GFP in HEK293, a human kidney cell line, resulted in perinuclear localization. To examine the membrane orientation of HRG-3, we conducted fluorescence protease protection (FPP) assays (Lorenz et al., 2006). In this procedure transfected cells are sequentially exposed to digitonin to permeabilize the cells, followed by protease digestion to cleave cytoplasmic-located proteins. For example, the membrane protein prototype, CFP-CD3δ-YFP, which is targeted to the endoplasmic reticulum (ER), contains a cytoplasmic YFP domain that is susceptible to protease digestion compared to the lumenal CFP domain, which remains intact (Figure 3E, upper panels). We found that HRG-3-GFP in transfected cells was not digested by the protease treatment, a result that was reproducible when the N-terminal 29 amino acids of HRG-3 (HRG-3N)

were expressed as a YFP fusion protein (Figure 3E). These results indicate that the C terminus of HRG-3 is protected from protease digestion and is not cytoplasmic.

To further identify the location of HRG-3 and the function of the N-terminal region, we synthesized truncated forms of HRG-3. Ectopic expression of these fusion proteins in HEK293 cells revealed that full-length HRG-3 and HRG-3N colocalized with the Golgi marker β 1,4-galactosyltransferase (GalT)-CFP, consistent with the localization of HRG-3 in the *C. elegans* intestinal cells (Figure 3F). However, deletion of the first 29 amino acids (HRG-3ΔN) resulted in a cytoplasmic localization, indicating that this N-terminal region is necessary for targeting HRG-3 to the secretory pathway. The localization of HRG-3 was not due to a large fluorescent protein tag because an HA epitope-tagged HRG-3 also colocalized with the GalT marker (Figure 3F, right panel), and coexpression of HRG-3-YFP and HRG-3-HA in the same cell resulted in both proteins colocalizing with the GalT marker (not shown).
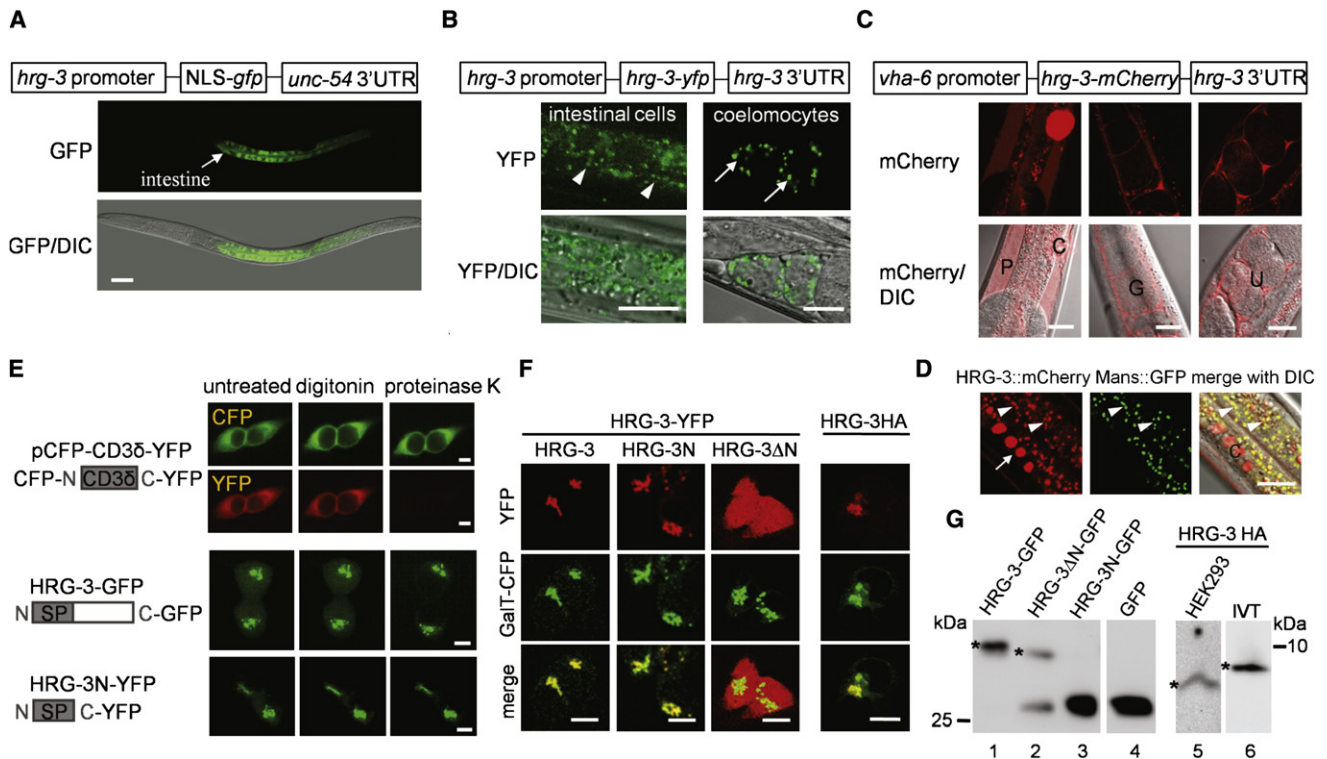
Figure 3. HRG-3 Is Secreted from the Maternal Intestine

(A) IQ8031 harboring the transcriptional reporter *Phrg-3::GFP* was maintained at 2 μM heme in axenic mCeHR-2 medium. Arrow indicates GFP expression in the intestine. Scale bars, 20 μm.

(B) Transgenic worms with the translational reporter *Phrg-3::HRG-3::YFP* were grown at 2 μM heme in axenic mCeHR-2 medium. YFP localization was examined at day 4 by confocal microscopy. Arrowhead, Golgi apparatus in the intestine; Arrow, coelomocytes. Scale bars, 10 μm.

(C) HRG-3::mCherry was expressed using an intestine-specific *vha-6* promoter and analyzed by confocal microscopy. HRG-3::mCherry was observed in coelomocytes (C), pseudocoelom (P), gonads (G), and uterus (U). Scale bars, 20 μm.

(D) The HRG-3::mCherry transgenic strain was crossed into strain RT1315, which expresses the Golgi-localized mannosidase (Mans)-GFP fusion protein. Images from these double transgenic worms were acquired by confocal microscopy. Arrowhead, Golgi apparatus in the intestine; Arrow and C, coelomocytes. Scale bars, 5 μm.

(E) Fluorescence protease protection assays in transfected HEK293 cells treated with digitonin and proteinase K. Time-lapse images were acquired in live cells by epifluorescence microscopy. Scale bars, 10 μm.

(F) Fluorescence (YFP) and immunofluorescence (HA) analyses of HRG-3 constructs in HEK293 cells. Galactosyltransferase (GalT)-CFP was used as a Golgi marker. Scale bars, 10 μm.

(G) Immunoblots of HRG-3 constructs. Left panel shows western blots of HRG-3 proteins expressed in HEK293 cells and probed with GFP antibody. Right panel shows the western blot of HRG-3-HA expressed either in HEK293 cells (lane 5) or in an in vitro transcription and translation system (IVT, lane 6) and probed with a HA antibody. The size difference between HRG-3-GFP (lane 1) and HRG-3ΔN::GFP (lane 2, top band) is ~0.4 kDa and between HRG-3N-GFP (lane 3) and GFP (lane 4) is <0.1 kDa. Lane 2 contains HRG-3 fusion protein (asterisk) and a smaller degradation product.

See also related Figure S2.

To examine whether the N terminus is cleaved or retained in HRG-3, transfected HEK293 cell lysates were subjected to analysis by SDS-PAGE and immunoblotting. The full-length HRG-3 and the HRG-3ΔN proteins were found to be equivalent in size (Figure 3G, lanes 1 and 2). Correspondingly, expression of HRG-3N-GFP resulted in a protein that was indistinguishable from GFP alone in size, suggesting that the N-terminal hydrophobic region is cleaved to produce the mature HRG-3-GFP protein (Figure 3G, lanes 3 and 4). To verify this result, we compared the molecular weight of HRG-3 that was generated either by in vitro transcription and translation or by transfecting HEK293 cells. Immunoblotting with anti-HA antibody revealed that the in vitro generated protein had a larger molecular weight,

corresponding to the retention of the 25 amino acid leader peptide (Figure 3G, lanes 5 and 6). These observations suggest that the N-terminal portion of HRG-3 may be processed and removed in the mature protein.

Specific Regulators of the Secretory Pathway Direct HRG-3 Trafficking

To identify the membrane-trafficking components that regulate HRG-3 secretion from the intestine, we used RNAi-mediated depletion of 45 genes that encode regulators of endocytosis and secretion (Table S1) (Balklava et al., 2007). We found that depletion of 15 trafficking factors caused HRG-3::mCherry to either accumulate within the maternal intestine (*vha-1*) or

Table 1. Regulators of Membrane Trafficking that Affect HRG-3-mCherry Expression and Localization

| Gene ID[a] | Name | Expression of HRG-3-mCherry | | |
		Intestine	Embryo	Extraintestinal
K02D10.5	snap-29	Increased	Increased	nc
T20G5.1	chc-1	Increased	Increased	nc
Y49A3A.2	vha-13	Increased	nc	nc
Y113G7A.3	sec-23	Increased	Increased	Lumenal
F12F6.6	sec-24.1	Increased	Increased	nc
R10E11.8	vha-1	Increased	nc	nc
Y25C1A.5	—	Increased	na	Lumenal
T01H3.1	vha-4	Increased	nc	nc
ZK970.4	vha-9	Increased	nc	nc
F59E10.3	—	Increased	na	Lumenal
R10E11.2	vha-2	Increased	nc	nc
Y55H10A.1	vha-19	Increased	nc	nc
ZK180.4	sar-1	Increased	nc	nc
F38E11.5	—	Increased	na	Lumenal
T14G10.5	—	Increased	nc	nc

na: these worms did not develop to the gravid stage.
nc: no change.
[a] List of positive genes compiled from Table S1.

mislocalize in extraintestinal tissues (sec-23) or embryos (sec-24.1) (Table 1 and Figure 4A). The majority of these candidate genes encoded for protein subunits that formed vesicle coatomer and vacuolar ATPase complexes (Table S1).

To determine whether HRG-3 secretion was tissue dependent, we ectopically expressed hrg-3::mCherry in the hypodermis, specialized epithelial cells in C. elegans, using the dpy-7 promoter (Rolls et al., 2002). Transgenic worms expressing Pdpy-7::HRG-3::mCherry revealed HRG-3::mCherry signal within cytoplasmic puncta in the hypodermis and in extrahypodermal cells including coelomocytes, the pseudocoelom, and the uterus (Figure 4B and Figure S3). As observed for the regulation of HRG-3 trafficking in the intestine, HRG-3 secretion from the hypodermis was also regulated by general membrane-trafficking components (Figure 4A versus Figure S3). Collectively, these results indicate that HRG-3 trafficking is mediated by general regulatory factors within the secretory pathway and is cell-type independent.

To examine whether HRG-3 secretion was dependent on organismal heme levels, we generated transgenic worms that expressed hrg-3::YFP under the control of the inducible hsp-16.2 promoter, which is strongly expressed in the intestine and induced in response to heat shock. HRG-3::YFP accumulated in the coelomocytes, which is indicative of secretion from the intestine, within 60 min after induction and continued to accumulate over time (Figures 4C and 4D). Importantly, Phsp-16.2::HRG-3::YFP transgenic worms accumulated similar amounts of HRG-3::YFP irrespective of heme concentrations in the growth medium (Figure 4E). We were unable to examine HRG-3::YFP secretion in worms grown at <1 μM heme because these animals were severely growth retarded.

To directly demonstrate that maternal HRG-3 is deposited within the embryo, we analyzed Pvha-6::HRG-3::mCherry mosaic transgenic worms in which the transgene was maintained as an extrachromosomal array with a transmission efficiency of ~60%. Thus, P_0 mothers that express HRG-3::mCherry will lay F_1 progeny that either express or lack the transgene (Figure 4F). Remarkably, 100% of F_1 embryos isolated from transgenic mothers were positive for HRG-3::mCherry even though 40% of these embryos did not express the transgene. HRG-3::mCherry was visible at the time of gastrulation and detectable up to the mid-larval stages (L2 and early L3). Importantly, 100% of the F_2 progeny, derived from nontransgenic HRG-3::mCherry-positive F_1 mothers, lacked any detectable HRG-3::mCherry signal and the transgene (Figure 4F). These results confirm that maternal HRG-3 is transferred to all embryos irrespective of the zygotic genotype.

Maternal HRG-3 Rescues the Growth Phenotypes

Our studies reveal that although hrg-3 is expressed in the intestine, hrg-3 loss-of-function mutants show embryonic lethality and growth retardation in the F_1 generation when grown under heme-insufficient conditions. These phenotypes could be due to HRG-3 deficiency either in P_0 mother, in the F_1 embryo, or both. To answer this question, we created a Phrg-3::HRG-3::ICS::GFP construct in which hrg-3 and gfp were under the control of a single hrg-3 promoter but were separated by the SL2 intercistronic sequence (ICS) from rla-1 (Figure 5A). In C. elegans, the HRG-3::ICS::GFP transgene is transcribed as a single polycistronic mRNA but yields two separate proteins: HRG-3 and GFP. Thus, GFP fluorescence is indicative of transgene expression (Figure 5A). Size and optical density analysis of stably transformed worms using a COPAS Biosort provided data that demonstrated that hrg-3 expression fully rescues the severe growth phenotype in the F_1 progeny in hrg-3-deficient worms in the presence of low heme (Figure 5B).

To confirm that intestinal HRG-3 is crucial for heme delivery to extraintestinal tissues, we used targeted gene rescue by expressing hrg-3 under the control of the intestine-specific vha-6 promoter. Unlike the hrg-3 promoter the vha-6 promoter is not heme regulated. Furthermore, to distinguish between maternal versus zygotic expressed HRG-3, we analyzed mosaic transformants in which the transgene transmission efficiency was ~40%. Thus, only P_0 mothers that express HRG-3::ICS::GFP will lay progeny that either lack hrg-3 or express hrg-3 as an extrachromosomal array. As expected, in the presence of low heme, >30% embryos from hrg-3 loss-of-function mothers failed to hatch and larvae that did hatch were growth arrested at the L1 stage. By contrast, <2% of embryos remained unhatched from P_0 mothers expressing the hrg-3 transgene (Figure 5C). Importantly, a significant proportion of hatched embryos derived from hrg-3-expressing mothers continued to grow past the L2 stage, even though these larvae did not express hrg-3 (Figure 5D and Figure 5E, center and right panels). hrg-3-expressing embryos derived from crosses between hrg-3 loss-of-function mothers and HRG-3::ICS::GFP males were growth arrested. Only 2 out of 65 F_1 progeny grew beyond the initial larval stages (Figures 5F and 5G). These data strongly suggest that targeted expression of hrg-3 from the maternal intestine is necessary
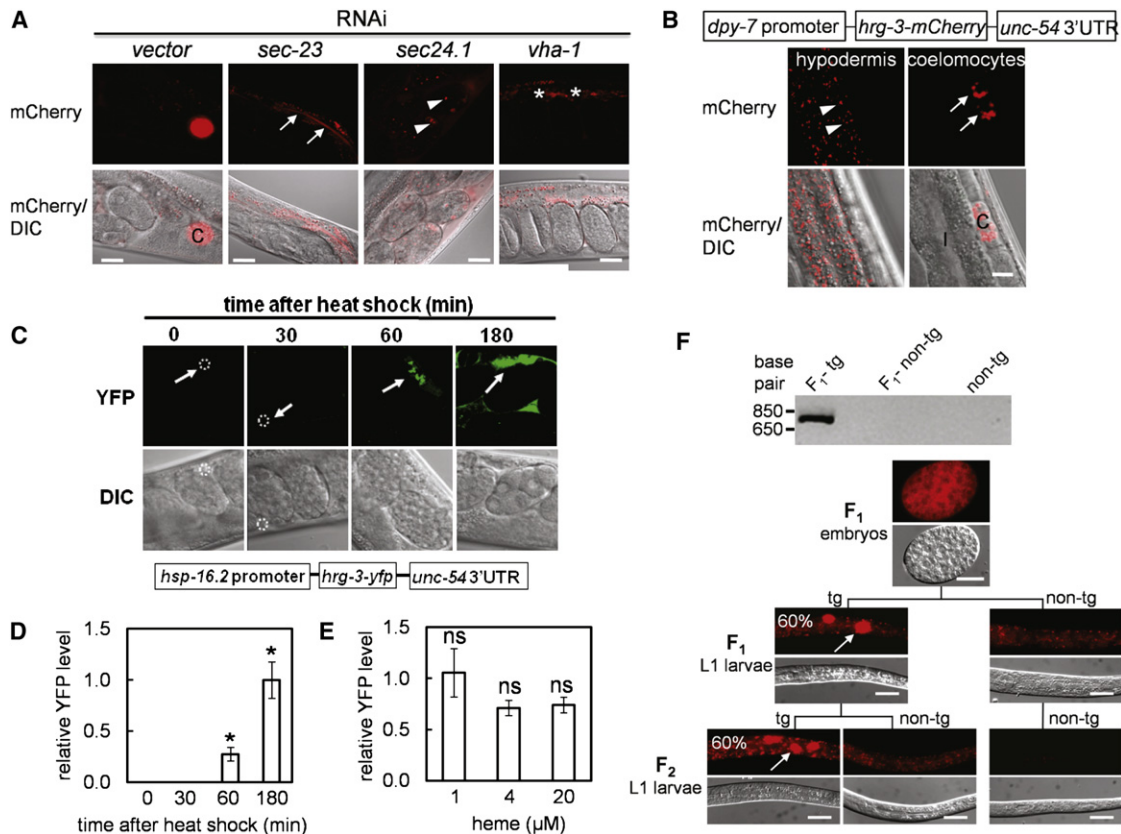
Figure 4. Regulators of the Secretory Pathway Direct HRG-3 Trafficking from the Maternal Intestine into the Embryos

(A) Depletion of candidate genes, selected from Table 1, alters HRG-3::mCherry expression in the intestine. RNAi against *sec-23* and *sec-24.1* resulted in accumulation of HRG-3::mCherry in the intestinal lumen (arrows) and the embryos (arrowheads), respectively. Asterisks indicate the increased HRG-3-mCherry level in the intestine due to *vha-1* depletion. C, coelomocytes. Scale bars, 20 μm.

(B) HRG-3::mCherry was expressed using a hypodermis-specific *dpy-7* promoter. Confocal images of the same cross-section but different focal planes are shown to distinguish hypodermal cells from coelomocytes (C). *Pdpy-7*::HRG-3::mCherry construct is not expressed in the intestine (I). Arrowhead, Golgi apparatus in the hypodermis; Arrows, coelomocytes. Scale bar, 10 μm.

(C) *C. elegans* expressing HRG-3::YFP under control of the *hsp-16.2* promoter were heat shocked at 37°C for 30 min and then transferred to 20°C for 0, 30, 60, or 180 min. Representative confocal images of YFP and DIC are shown. Dotted circles in the first two images and arrows indicate the position of coelomocytes. Scale bars, 20 μm.

(D) Quantification of HRG-3::YFP secretion from the intestine by measuring accumulation in coelomocytes at different time points after a 30 min induction by heat shock. Asterisks indicate that this group is statistically different from any other groups (p < 0.001). Error bars indicate SEM from two independent experiments.

(E) Worms carrying *Phsp-16.2*::HRG-3::YFP grown on RP523 bacteria supplemented with 1, 4, or 20 μM heme for 72 hr were heat shocked at 37°C for 30 min. Worms were transferred to 20°C for 60 min and YFP intensity in coelomocytes was quantified and normalized to the coelomocyte volume. *ns*, not significant (p > 0.05). Error bars indicate SEM from two independent experiments.

(F) Progeny derived from *Pvha-6::HRG-3::mCherry* mosaic transgenic worms with a transmission efficiency of ~60% were analyzed by epifluorescence microscopy for two successive generations. Representative images of transgenic (tg) and nontransgenic (non-tg) L1 larvae are shown. Numbers represent the percentage of segregating progeny that contain the HRG-3::mCherry transgene. Although 100% of the embryos were positive for HRG-3::mCherry, in each generation only ~60% of the L1 progeny were transgenic. A hallmark of these transgenic worms was the accumulation of HRG-3::mCherry in coelomocytes (arrows). Scale bars, 20 μm. Genotypes were confirmed in single worms by PCR amplification of the mCherry transgene using genomic DNA template (top panel). See also related Figure S3.

and sufficient for embryonic development even when environmental heme is limiting.

hrg-3 Mutant Embryos Have Reduced Heme Levels

Our results support a role for HRG-3 in heme delivery from the maternal intestine to oocytes. Based on this evidence, we postulated that when HRG-3 is available in limited quantities, greater heme accumulation would be found in the maternal intestine and a corresponding heme deficiency would exist in the developing embryos compared to wild-type worms. To estimate heme levels in these tissues, we crossed the heme sensor strain IQ6011 (*Phrg-1::GFP*) with *hrg-3* null mutants (Rajagopal et al., 2008; Severance et al., 2010; Sinclair and Hamza, 2010). The resulting IQ8011 gravid worms had reduced GFP levels in the intestine compared to IQ6011 worms (control) when grown in medium containing 1.5 or 2 μM heme (Figure 6A). Embryos derived from these mothers showed reproducibly higher levels of GFP, compared to wild-type controls (Figure 6B). As the
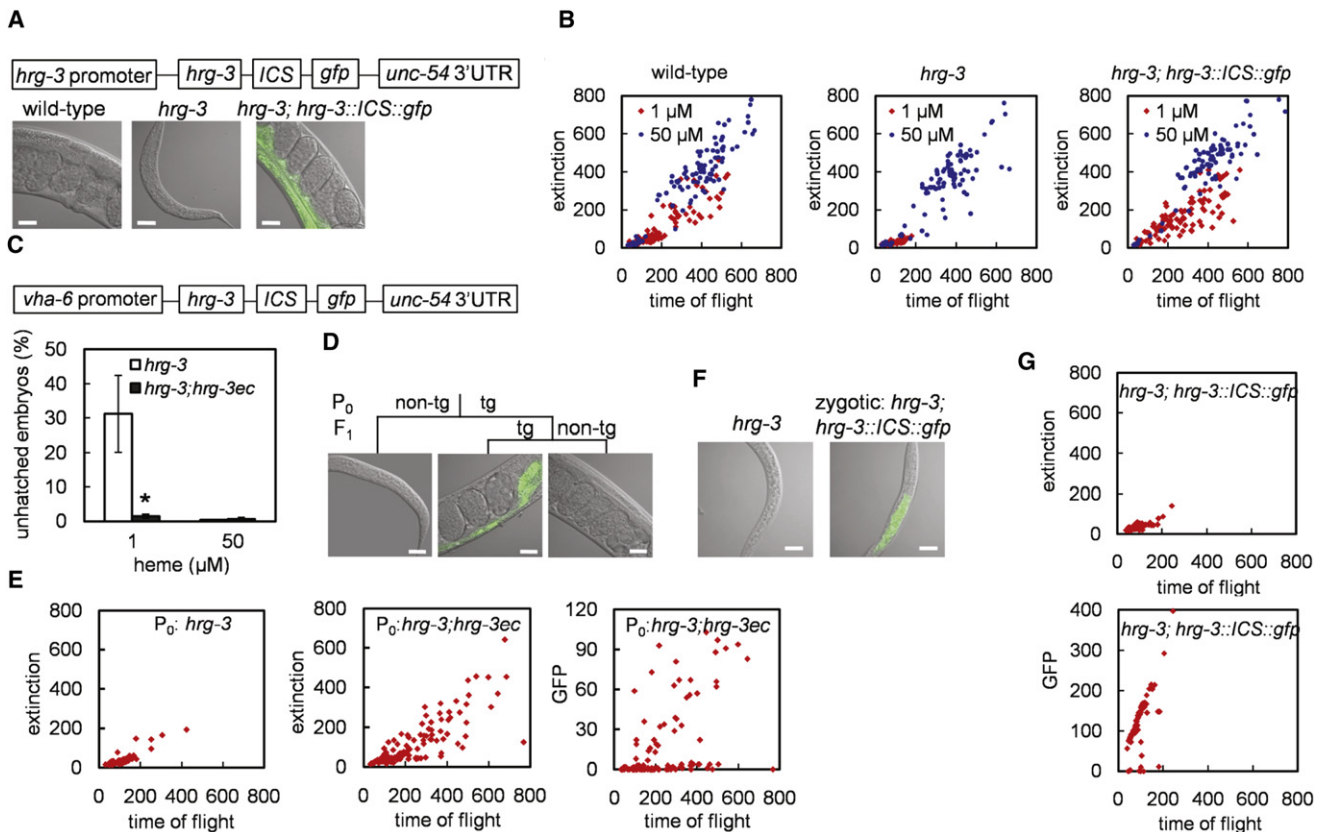
Figure 5. Maternal Expression of *hrg-3* Is Sufficient to Rescue the Early Embryonic Growth Phenotype

(A) *hrg-3* and *gfp* were expressed using a single *hrg-3* promoter but were separated by the intercistronic sequence (ICS) from *rla-1*. Introduction of this construct into *hrg-3* null mutant restored the growth of F$_1$ progeny at low heme. Progeny grown on RP523 with 1 μM heme were photographed at day 6 post-hatching. Representative images of arrested or rescued F$_1$ worms are presented. Scale bar, 20 μm.

(B) Worm strains were grown on RP523 with 1 and 50 μM heme for two subsequent generations. The sizes of the F$_1$ worms were measured by COPAS BioSort. Time of flight and extinction indicate the length and the optical density of worms, respectively.

(C) The *HRG-3::ICS::GFP* construct (*hrg-3ec*) was expressed using an intestinal-specific *vha-6* promoter. A transgenic strain with ∼40% transmission efficiency was crossed to the *hrg-3* mutant. GFP-expressing mothers gave rise to >98% live progeny at low heme. Error bars indicate the SEM from three individual experiments. *p < 0.05 compared with *hrg-3* mutant under the same condition.

(D) *hrg-3* mutant worms with or without *hrg-3ec* construct were grown on RP523 with 1 μM heme for one generation. Their progeny were maintained under the same condition for 5 days. Representative images of the arrested and rescued progeny are presented. "tg" and "non-tg" denote whether the *hrg-3* null mutants express or lack *hrg-3ec* construct, respectively. Scale bars, 20 μm.

(E) Progeny from Figure 5D were sorted based on size (extinction) and transgene (GFP) by COPAS BioSort.

(F) *HRG-3::ICS::GFP* males were crossed with *hrg-3* mutant hermaphrodites that had been grown on RP523 supplemented with 1 μM heme for one generation. The F$_1$ heterozygous progeny were maintained at the 1 μM heme for 5 days. Representative images of the arrested progeny are shown. Scale bars, 20 μm.

(G) F$_1$ progeny from (F) were sorted based on size (extinction) and transgene (GFP) by COPAS BioSort.

heme status is inversely correlated with the GFP expression in heme sensor worms, these results suggest that deletion of *hrg-3* results in increased heme levels in the maternal intestine and reduced heme levels in the embryos. The modest differences in embryonic GFP levels between wild-type and *hrg-3* embryos could be due to incomplete penetrance of the embryonic lethal phenotype (∼40%; Figure 2C and Figure 5C) and environmental modifiers such as nutrient heme (Figure 2C). The consistently higher GFP (∼5 fold) content in the intestine of the mother compared to the embryo could be attributed to the endoreduplication of chromosomes and multi-nucleation of the intestinal cells during worm development (Hedgecock and White, 1985). Taken together, our results show that HRG-3

deficiency causes perturbation of heme homeostasis in the maternal intestine and the embryo.

HRG-3 Is a Heme-Binding Protein

Although the genetic and cell biology data are compelling in demonstrating that HRG-3 is involved in trafficking of heme from the maternal intestine to eggs, the data do not discriminate between direct or indirect functions of HRG-3 in heme homeostasis. To determine whether HRG-3 directly interacts with heme, we synthesized the mature secreted form of HRG-3 and measured its ability in vitro to bind heme. Pure HRG-3 is readily soluble in weak acidic solutions but becomes less soluble and gradually precipitates at neutral pH. However, addition of ferric
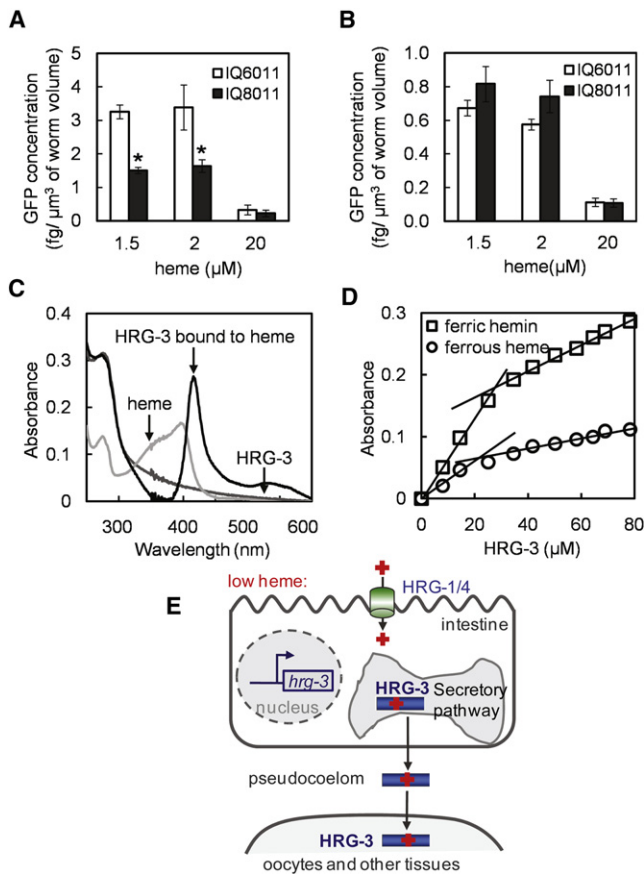
Figure 6. Maternal-to-Embryonic Heme Transfer Is Perturbed in *hrg-3* Mutant Worms

(A) The IQ8011 (*hrg-3*; *Phrg-1::GFP*) strain was generated by crossing the *hrg-3* mutant into the heme sensor IQ6011 strain. Both strains were maintained in axenic mCeHR-2 medium with the indicated heme concentrations for 4 days. GFP levels were measured by fluorimetry in protein lysates prepared from the gravid adults. Error bars indicate the SEM from four individual experiments. *p < 0.01 compared with *hrg-3* mutants under the same conditions.

(B) IQ6011 and IQ8011 worms were maintained in axenic mCeHR-2 medium with the indicated heme concentrations for 4 days. F_1 embryos obtained by bleaching the gravid adults were homogenized and GFP levels measured by fluorimetry. Error bars indicate the SEM from four individual experiments.

(C) Absorption spectra of HRG-3 peptide in the presence or absence of heme, and free heme alone in buffer without added HRG-3. Heme-bound HRG-3 displays an absorbance peak at ∼416 nm, which is clearly shifted in both wavelength and intensity from that of free heme.

(D) Absorption spectra of HRG-3 peptide in the presence of ferric or ferrous heme. Increasing amounts of HRG-3 were added to 9 μM ferric heme or ferrous heme (in the presence of dithionite), and the absorbance was monitored at 415 nm or 441 nm, respectively.

(E) The proposed model of HRG-3 as a heme chaperone. Heme deficiency induces the expression of HRG-1 and HRG-4, membrane-bound permeases that import heme (red cross) into the intestine, and HRG-3, which is secreted from the intestine into the circulatory system (pseudocoelom) for heme delivery to extraintestinal cells.

protoheme to a solution of soluble HRG-3 at pH 7.0 resulted in a distinct spectroscopic peak at 416 nm (Figure 6C), whereas addition of ferrous protoheme resulted in a peak at 441 nm

(not shown). These peaks are shifted and distinct from those of the free heme, indicating that heme is definitively binding HRG-3. Although we were unable to obtain an accurate association constant spectroscopically because the binding affinity of HRG-3 for heme was weak, titration of both ferric and ferrous heme revealed that, regardless of oxidation state, heme binds to HRG-3 at a stoichiometry of 1:2 (heme:protein) (Figure 6D). Notably, the soluble heme-bound HRG-3 slowly precipitates over several hours as a bright red complex, indicating that the precipitated protein remains bound to heme with significant affinity.

DISCUSSION

As a heme auxotroph, embryonic and postembryonic development in *C. elegans* is dependent on either maternal heme deposition (Figure 1A, upper panel) or larval heme acquisition (Figure 1A, lower panel). Our results uncover the crucial role of HRG-3 in maintaining embryonic heme homeostasis and its interdependence with maternal heme status (Figures 2C–2E and Figures 5C–5E). *C. elegans* acquires environmental heme through the coordinated functions of HRG-1 membrane-bound heme permeases located in the intestine (Rajagopal et al., 2008). Because a hermaphrodite worm has 959 somatic cells of which 20 are polarized intestinal cells (McGhee, 2007), the question remaining is how do extraintestinal cells acquire heme? We postulate that this is partly accomplished through HRG-3, which we have shown above is likely to be an intercellular heme chaperone (Figure 6E). HRG-3 is transcriptionally upregulated in response to heme insufficiency and secreted by the maternal intestine into the pseudocoelom, the worm's circulatory system, for mobilization of heme to extraintestinal tissues including the gonads and uterus. In the absence of HRG-3, heme accumulates in the intestine of gravid adults, whereas the embryos are heme deficient resulting in embryonic lethality or growth arrest immediately after the embryos hatch.

When and how does HRG-3 transfer heme to the embryo? In *C. elegans*, oocyte fertilization results in a rapid assembly of a trilamellate chitinous eggshell by the time pseudocleavage of the one-cell embryo occurs (Johnston et al., 2006). The eggshell, which surrounds the developing embryo until hatching, provides a mechanical and osmotic barrier and ensures that early developmental events occur (Johnston et al., 2006). Given the impervious nature of the eggshell matrix to environmental factors, we speculate that heme deposition by HRG-3 must occur during oocyte maturation and prior to fertilization. This maternal-to-oocyte trafficking of heme exhibits striking similarity with the lipid transport pathways by vitellogenins, the major yolk precursor proteins. *C. elegans* contains six vitellogenins that are produced by the maternal intestine to bind lipids and translocated to the gonads via the pseudocoelom for yolk deposition in oocytes (Blumenthal et al., 1984; Kimble and Sharrock, 1983; Spieth and Blumenthal, 1985). However, unlike vitellogenins that are expressed only in the adult hermaphrodite (Blumenthal et al., 1984), *hrg-3* is expressed during all developmental stages in both hermaphrodites and males (Figure S2). HRG-3 may, therefore, play a more extensive role than vitellogenins by mobilizing heme from intestinal cells to tissues other than embryos. Indeed,

HRG-3-deficient F_1 larvae are growth arrested in the presence of low heme, implying that, in addition to in utero development that can be rescued by maternal HRG-3, sustained *hrg-3* expression in the larvae is essential for postembryonic development. A similar pathway may also exist for other metals such as zinc, which has been recently demonstrated to regulate meiotic maturation of mammalian oocytes and early embryonic development, implicating a role for zinc in the maternal legacy from egg to embryo (Kim et al., 2010).

What are the cellular factors that regulate HRG-3 trafficking? Of the 45 general regulators of membrane trafficking that were recently identified from a genome-wide RNAi screen for modulators of endocytosis and secretion of vitellogenin (Balklava et al., 2007), RNAi depletion of 15 factors caused HRG-3 to accumulate or mislocalize in both the intestine and hypodermis (Table 1). Interestingly, these regulators broadly fall into two categories—coatomer complex and vacuolar ATPase subunits. HRG-3 trafficking and secretion may therefore be dependent on assembly of vesicles and its acidification. Although maternal HRG-3 persists from embryonic to larval stages, just like vitellogenin (Chotard et al., 2010), HRG-3 is not part of the vitellogenin complex because RNAi depletion of all six vitellogenins did not alter HRG-3 secretion and trafficking (not shown). There are several examples of maternal contributions to the embryo that persist and function at later stages of development. For example, maternal cyclin E, a cell-cycle checkpoint regulator, controls G_1/S progression and coordinates cell proliferation and differentiation in *C. elegans* (Brodigan et al., 2003; Fay and Han, 2000). Maternal cyclin E is sufficient to regulate G1 cell-cycle progression until the L3/L4 larval stages; cell-cycle defects only become apparent when the maternal protein is exhausted in the F_1 progeny.

Our biochemical studies demonstrate that the mature processed HRG-3 protein binds both ferrous and ferric heme with an apparent stoichiometry of two protein and one heme moiety. The spectroscopic data are consistent with a five coordinate high spin heme and reproducible by electron paramagnetic resonance spectroscopy (A.N. Albetel, M.K. Johnson, H.A.D., and I.H., unpublished data). We propose that heme transfer by HRG-3 to target sites may be dependent on affinity gradients, as has been demonstrated for intracellular copper chaperones. Copper transfer is thermodynamically favored from low- to intermediate- to high-affinity sites driven by intracellular metallochaperones; the hierarchy of copper binding among specific chaperones is governed by fast metal transfer, specific protein-protein recognition, and cellular compartmentalization (Banci et al., 2010).

Although intercellular transport of iron by the transferrin-transferrin receptor complex has been well documented, several lines of evidence also support the existence of an intercellular heme transport pathway in vertebrates. First, even though knockout of the heme synthesis pathway in mice is embryonic lethal, homozygous embryos survive at least until embryonic day (E) 3.5, suggesting the existence of heme stores (Magness et al., 2002; Okano et al., 2010). Second, zebrafish embryos with loss-of-function mutations in heme synthesis genes can survive from 10–25 days post-fertilization (Childs et al., 2000; Dooley et al., 2008), plausibly because these embryos may

contain either maternal-derived mRNA for heme synthesis enzymes or direct deposition of maternal heme. Third, human patients with acute attacks of porphyrias, genetic diseases due to defects in heme synthesis enzymes, are administered heme intravenously as an effective therapeutic treatment, which results in reduction of heme synthesis intermediates and a concomitant increase in liver heme-dependent enzyme activities for cytochrome P450 and tryptophan 2,3-dioxygenase, indicating that infused heme in the blood stream is utilized in toto by peripheral tissues (Puy et al., 2010; Bonkovsky et al., 1991). Lastly, cell culture studies with human colon-derived Caco-2 cells and mouse macrophages reveal that a portion of heme, derived from dietary sources or senescent red blood cells, is released into the blood stream as an intact metalloporphyrin (Knutson et al., 2005; Uc et al., 2004). A potential candidate for an intercellular heme delivery protein would be hemopexin, which scavenges heme with an apparent dissociation constant (K_D) $\sim 10^{-15}$ M and clears it from the circulatory system (Hrkal et al., 1974). The heme-hemopexin complex binds to the LRP/CD91 receptor and is endocytosed, and the majority of the hemopexin is degraded in the endo-lysosome of hepatocytes, macrophages, and syncytiotrophoblasts (Hvidberg et al., 2005; Tolosano et al., 2010). Surprisingly, hemopexin null mice are viable and fertile and present no evidence of tissue damage due to oxidative stress from abnormal heme and/or iron deposition under normal conditions; heme overload and hemolytic damage, however, cause tissue damage in these mice (Tolosano et al., 1999, 2010). We speculate that a functional homolog of HRG-3 may also exist in vertebrates as an alternate pathway to facilitate the targeted delivery and redistribution of heme between tissues and specific cell types and maintain systemic heme homeostasis.

Even though heme uptake and transport pathways are clearly conserved across metazoans (Severance and Hamza, 2009), heme auxotrophic organisms, such as *C. elegans* and parasitic helminthes, are crucially dependent on these pathways for utilization of environmental heme for growth and reproduction (Rao et al., 2005). Helminths affect more than a quarter of the world's population (Chan et al., 1994; Hotez et al., 2008) and cause tens of billions of dollars of loss in animal and plant production annually (Fuller et al., 2008; Jasmer et al., 2003). Moreover, anthelminthics are becoming less effective in humans and livestock because of rampant drug resistance (Fuller et al., 2008; Jasmer et al., 2003). We propose that an excellent anthelminthic target would be the HRG-3-mediated pathway for transporting heme to developing oocytes, especially in parasites such as hookworms, which infect more than a billion people worldwide and feed on host red blood cell hemoglobin (Held et al., 2006; Wu et al., 2009).

EXPERIMENTAL PROCEDURES

Worm Growth Assays on *RP523*

The heme-deficient *E. coli* strain RP523 was maintained in liquid LB medium supplemented with 1 μM heme at 37°C (Li et al., 1988). To prevent unequal growth of the RP523, overnight cultures were diluted into fresh medium with different concentrations of heme, grown for 5.5 hr, and heat inactivated at 65°C for 2–5 min. A 0.2 optical density (OD) 600 of bacteria was seeded on each 35 mm nematode growth medium (NGM) agar plate. Synchronized L1

larvae of *hrg-3* (*tm2468*) allele and its wild-type broodmates were placed onto RP523 plates and incubated at 20°C for 3–5 days. Five gravid hermaphrodites from each plate were allowed to lay eggs for 12–16 hr on a new RP523 seeded plate. The embryos that did not hatch after 24–32 hr were considered dead. The growth of F_1 larvae was scored when the wild-type worms reached young adult stage. Those larvae that did not progress past L2 stage were considered growth arrested. DIC images were acquired on the F_1 worms when the wild-type broodmates reached gravid stage.

Worm Analysis with COPAS BioSort

Nematodes from plates containing RP523 were frozen when worms reached gravid stage. Worms from each sample (∼100) were analyzed for length (time of flight) and optical density (extinction) by using a COPAS BioSort (Union Biometrica, Holliston, MA, USA). Gating parameters of time of flight 30–800 and extinction 15–800 were set by using synchronized L1s and mixed worm populations. Raw data outside this range were filtered to exclude particulates and bubbles. For rescue experiments, *hrg-3* mutants expressing *Phrg-3::HRG-3::ICS::GFP* (integrated) or *Pvha-6::HRG-3::ICS::GFP* (extra-chromosomal array) were generated by genetic crosses. For zygotic rescue experiment, *hrg-3* mutants were grown on RP523 with 1 μM heme for one generation, followed by crossing with male worms expressing *Phrg-3::HRG-3::ICS::GFP*. The progeny were maintained at low heme for 5 days. Both worm size and GFP intensity were analyzed using COPAS BioSort for maternal and zygotic rescue experiments. The settings for GFP measurements in the zygotic rescue experiments were gain = 3.5 and PMT voltage = 750 but for all other experiments the settings were gain = 3.0 and PMT voltage = 600.

Maternal Transfer of HRG-3::mCherry

C. elegans transmitting the transgene *Pvha6*::HRG-3::mCherry with 60% efficiency to its progeny were grown on NGM plates seeded with RP523 supplemented with 4 μM heme. Embryos from adult gravid worms either with or without the transgene were released from the uterus using a needle. These embryos were analyzed for mCherry expression using a Leica DMIRE2 inverted microscope and Simple PCI software. In parallel, transgenic P_0 gravid worms were individually picked onto new plates and allowed to produce F_1 progeny and analyzed for mCherry expression by epifluorescence microscopy. These F_1 worms were separated and grown till they lay F_2 progeny, which were analyzed for the mCherry transgene.

Fluorescence Protease Protection Assay

The procedure for fluorescence protease protection (FPP) assay was modified from the protocol of Lorenz et al. (2006). HRG-3-GFP and control plasmid pCFP-CD3δ-YFP were transfected into HEK293 cells grown on Lab-Tek chambered coverglass (Nunc). After 24 hr, the cells were washed with KHM buffer (110 mM potassium acetate, 2 mM $MgCl_2$, and 20 mM HEPES, pH 7.3), and the cell chambers were moved to a DMIRE2 epifluorescence microscope (Leica) connected to a Retiga 1300 cooled Mono 12-bit camera. Time-lapse images were acquired before and after digitonin treatment (30 μM digitonin/2 min) and following proteinase K (50 μg/ml) digestion.

Statistical Analysis

All data are presented as mean ± standard error of the mean (SEM). Statistical significance was tested using one-way ANOVA followed by the Tukey-Kramer Multiple Comparisons Test in GraphPad INSTAT version 3.01 (GraphPad, San Diego, CA, USA). A p value of < 0.05 was considered as statistically significant.

Additional material is available in the Extended Experimental Procedures.

SUPPLEMENTAL INFORMATION

Supplemental Information includes Extended Experimental Procedures, three figures, and two tables and can be found with this article online at doi:10.1016/j.cell.2011.04.025.

REFERENCES

Balklava, Z., Pant, S., Fares, H., and Grant, B.D. (2007). Genome-wide analysis identifies a general requirement for polarity proteins in endocytic traffic. Nat. Cell Biol. *9*, 1066–1073.

Balla, G., Vercellotti, G.M., Muller-Eberhard, U., Eaton, J., and Jacob, H.S. (1991). Exposure of endothelial cells to free heme potentiates damage mediated by granulocytes and toxic oxygen species. Lab. Invest. *64*, 648–655.

Banci, L., Bertini, I., Ciofi-Baffoni, S., Kozyreva, T., Zovo, K., and Palumaa, P. (2010). Affinity gradients drive copper to cellular destinations. Nature *465*, 645–648.

Blumenthal, T., Squire, M., Kirtland, S., Cane, J., Donegan, M., Spieth, J., and Sharrock, W. (1984). Cloning of a yolk protein gene family from Caenorhabditis elegans. J. Mol. Biol. *174*, 1–18.

Bonkovsky, H.L., Healey, J.F., Lourie, A.N., and Gerron, G.G. (1991). Intravenous heme-albumin in acute intermittent porphyria: evidence for repletion of hepatic hemoproteins and regulatory heme pools. Am. J. Gastroenterol. *86*, 1050–1056.

Brodigan, T.M., Liu, J., Park, M., Kipreos, E.T., and Krause, M. (2003). Cyclin E expression during development in Caenorhabditis elegans. Dev. Biol. *254*, 102–115.

Chan, M.S., Medley, G.F., Jamison, D., and Bundy, D.A. (1994). The evaluation of potential global morbidity attributable to intestinal nematode infections. Parasitology *109*, 373–387.

Childs, S., Weinstein, B.M., Mohideen, M.A., Donohue, S., Bonkovsky, H., and Fishman, M.C. (2000). Zebrafish dracula encodes ferrochelatase and its mutation provides a model for erythropoietic protoporphyria. Curr. Biol. *10*, 1001–1004.

Chotard, L., Skorobogata, O., Sylvain, M.A., Shrivastava, S., and Rocheleau, C.E. (2010). TBC-2 is required for embryonic yolk protein storage and larval survival during L1 diapause in Caenorhabditis elegans. PLoS ONE *5*, e15662.

Dailey, H.A. (2002). Terminal steps of haem biosynthesis. Biochem. Soc. Trans. *30*, 590–595.

Dooley, K.A., Fraenkel, P.G., Langer, N.B., Schmid, B., Davidson, A.J., Weber, G., Chiang, K., Foott, H., Dwyer, C., Wingert, R.A., et al; Tübingen 2000 Screen Consortium. (2008). montalcino, A zebrafish model for variegate porphyria. Exp. Hematol. *36*, 1132–1142.

Faller, M., Matsunaga, M., Yin, S., Loo, J.A., and Guo, F. (2007). Heme is involved in microRNA processing. Nat. Struct. Mol. Biol. *14*, 23–29.

Fay, D.S., and Han, M. (2000). Mutations in cye-1, a Caenorhabditis elegans cyclin E homolog, reveal coordination between cell-cycle control and vulval development. Development *127*, 4049–4060.

Fuller, V.L., Lilley, C.J., and Urwin, P.E. (2008). Nematode resistance. New Phytol. *180*, 27–44.

Hardison, R.C. (1996). A brief history of hemoglobins: plant, animal, protist, and bacteria. Proc. Natl. Acad. Sci. USA *93*, 5675–5679.

Hedgecock, E.M., and White, J.G. (1985). Polyploid tissues in the nematode Caenorhabditis elegans. Dev. Biol. *107*, 128–133.

Held, M.R., Bungiro, R.D., Harrison, L.M., Hamza, I., and Cappello, M. (2006). Dietary iron content mediates hookworm pathogenesis in vivo. Infect. Immun. *74*, 289–295.

Hotez, P.J., Brindley, P.J., Bethony, J.M., King, C.H., Pearce, E.J., and Jacobson, J. (2008). Helminth infections: the great neglected tropical diseases. J. Clin. Invest. *118*, 1311–1321.

Hrkal, Z., Vodrázka, Z., and Kalousek, I. (1974). Transfer of heme from ferrihemoglobin and ferrihemoglobin isolated chains to hemopexin. Eur. J. Biochem. *43*, 73–78.

Hvidberg, V., Maniecki, M.B., Jacobsen, C., Højrup, P., Møller, H.J., and Moestrup, S.K. (2005). Identification of the receptor scavenging hemopexin-heme complexes. Blood *106*, 2572–2579.

Jasmer, D.P., Goverse, A., and Smant, G. (2003). Parasitic nematode interactions with mammals and plants. Annu. Rev. Phytopathol. *41*, 245–270.

Johnston, W.L., Krizus, A., and Dennis, J.W. (2006). The eggshell is required for meiotic fidelity, polar-body extrusion and polarization of the C. elegans embryo. BMC Biol. *4*, 35.

Kaasik, K., and Lee, C.C. (2004). Reciprocal regulation of haem biosynthesis and the circadian clock in mammals. Nature *430*, 467–471.

Keel, S.B., Doty, R.T., Yang, Z., Quigley, J.G., Chen, J., Knoblaugh, S., Kingsley, P.D., De Domenico, I., Vaughn, M.B., Kaplan, J., et al. (2008). A heme export protein is required for red blood cell differentiation and iron homeostasis. Science *319*, 825–828.

Kim, A.M., Vogt, S., O'Halloran, T.V., and Woodruff, T.K. (2010). Zinc availability regulates exit from meiosis in maturing mammalian oocytes. Nat. Chem. Biol. *6*, 674–681.

Kim, B.E., Nevitt, T., and Thiele, D.J. (2008). Mechanisms for copper acquisition, distribution and regulation. Nat. Chem. Biol. *4*, 176–185.

Kimble, J., and Sharrock, W.J. (1983). Tissue-specific synthesis of yolk proteins in Caenorhabditis elegans. Dev. Biol. *96*, 189–196.

Knutson, M.D., Oukka, M., Koss, L.M., Aydemir, F., and Wessling-Resnick, M. (2005). Iron release from macrophages after erythrophagocytosis is upregulated by ferroportin 1 overexpression and down-regulated by hepcidin. Proc. Natl. Acad. Sci. USA *102*, 1324–1328.

Li, J.M., Umanoff, H., Proenca, R., Russell, C.S., and Cosloy, S.D. (1988). Cloning of the Escherichia coli K-12 hemB gene. J. Bacteriol. *170*, 1021–1025.

Lorenz, H., Hailey, D.W., and Lippincott-Schwartz, J. (2006). Fluorescence protease protection of GFP chimeras to reveal protein topology and subcellular localization. Nat. Methods *3*, 205–210.

Magness, S.T., Maeda, N., and Brenner, D.A. (2002). An exon 10 deletion in the mouse ferrochelatase gene has a dominant-negative effect and causes mild protoporphyria. Blood *100*, 1470–1477.

McGhee, J.D. (2007). The C. elegans intestine. WormBook, 1–36.

Oka, T., Toyomura, T., Honjo, K., Wada, Y., and Futai, M. (2001). Four subunit a isoforms of Caenorhabditis elegans vacuolar H+-ATPase. Cell-specific expression during development. J. Biol. Chem. *276*, 33079–33085.

Okano, S., Zhou, L., Kusaka, T., Shibata, K., Shimizu, K., Gao, X., Kikuchi, Y., Togashi, Y., Hosoya, T., Takahashi, S., et al. (2010). Indispensable function for

embryogenesis, expression and regulation of the nonspecific form of the 5-aminolevulinate synthase gene in mouse. Genes Cells *15*, 77–89.

Puy, H., Gouya, L., and Deybach, J.C. (2010). Porphyrias. Lancet *375*, 924–937.

Quigley, J.G., Yang, Z., Worthington, M.T., Phillips, J.D., Sabo, K.M., Sabath, D.E., Berg, C.L., Sassa, S., Wood, B.L., and Abkowitz, J.L. (2004). Identification of a human heme exporter that is essential for erythropoiesis. Cell *118*, 757–766.

Rajagopal, A., Rao, A.U., Amigo, J., Tian, M., Upadhyay, S.K., Hall, C., Uhm, S., Mathew, M.K., Fleming, M.D., Paw, B.H., et al. (2008). Haem homeostasis is regulated by the conserved and concerted functions of HRG-1 proteins. Nature *453*, 1127–1131.

Rao, A.U., Carta, L.K., Lesuisse, E., and Hamza, I. (2005). Lack of heme synthesis in a free-living eukaryote. Proc. Natl. Acad. Sci. USA *102*, 4270–4275.

Rolls, M.M., Hall, D.H., Victor, M., Stelzer, E.H., and Rapoport, T.A. (2002). Targeting of rough endoplasmic reticulum membrane proteins and ribosomes in invertebrate neurons. Mol. Biol. Cell *13*, 1778–1791.

Severance, S., and Hamza, I. (2009). Trafficking of heme and porphyrins in metazoa. Chem. Rev. *109*, 4596–4616.

Severance, S., Rajagopal, A., Rao, A.U., Cerqueira, G.C., Mitreva, M., El-Sayed, N.M., Krause, M., and Hamza, I. (2010). Genome-wide analysis reveals novel genes essential for heme homeostasis in Caenorhabditis elegans. PLoS Genet. *6*, e1001044.

Sinclair, J., and Hamza, I. (2010). A novel heme-responsive element mediates transcriptional regulation in Caenorhabditis elegans. J. Biol. Chem. *285*, 39536–39543.

Spieth, J., and Blumenthal, T. (1985). The Caenorhabditis elegans vitellogenin gene family includes a gene encoding a distantly related protein. Mol. Cell. Biol. *5*, 2495–2501.

Tolosano, E., Hirsch, E., Patrucco, E., Camaschella, C., Navone, R., Silengo, L., and Altruda, F. (1999). Defective recovery and severe renal damage after acute hemolysis in hemopexin-deficient mice. Blood *94*, 3906–3914.

Tolosano, E., Fagoonee, S., Morello, N., Vinchi, F., and Fiorito, V. (2010). Heme scavenging and the other facets of hemopexin. Antioxid. Redox Signal. *12*, 305–320.

Uc, A., Stokes, J.B., and Britigan, B.E. (2004). Heme transport exhibits polarity in Caco-2 cells: evidence for an active and membrane protein-mediated process. Am. J. Physiol. Gastrointest. Liver Physiol. *287*, G1150–G1157.

Worthington, M.T., Cohn, S.M., Miller, S.K., Luo, R.Q., and Berg, C.L. (2001). Characterization of a human plasma membrane heme transporter in intestinal and hepatocyte cell lines. Am. J. Physiol. Gastrointest. Liver Physiol. *280*, G1172–G1177.

Wu, B., Novelli, J., Foster, J., Vaisvila, R., Conway, L., Ingram, J., Ganatra, M., Rao, A.U., Hamza, I., and Slatko, B. (2009). The heme biosynthetic pathway of the obligate Wolbachia endosymbiont of Brugia malayi as a potential antifilarial drug target. PLoS Negl. Trop. Dis. *3*, e475.

Yang, Z., Philips, J.D., Doty, R.T., Giraudi, P., Ostrow, J.D., Tiribelli, C., Smith, A., and Abkowitz, J.L. (2010). Kinetics and specificity of feline leukemia virus subgroup C receptor (FLVCR) export function and its dependence on hemopexin. J. Biol. Chem. *285*, 28874–28882.